Steady State ECRH Operation at the W7-X Stellarator*)

Heinrich Peter LAQUA and the W7-X Team[1)]

Max-Planck-Institute for Plasma Physics EURATOM Association, Garching and Greifswald, Germany

[1)]*The author list of the W7-X Team is listed in [1]*

(Received 30 November 2020 / Accepted 24 February 2021)

The Steady state operation can be defined for various characteristic physical time scales. Usually one speaks of steady state plasmas when the discharges are stationary for several energy confinement times. The next longer time constant is the L/R time for the development of the toroidal plasma current. Ultimately, the gas equilibrium must also be achieved. W7-X is ideal for creating stationary conditions for the different plasma parameters. In the operation phase OP1.2, the experimental operation was neither limited by the confining magnetic field nor by the pulse length of the ECRH. Only the maximum tolerable temperature of the uncooled in-vessel components and the test divertor unit (TDU) limited the total input energy. Therefore this paper presents steady state operation different plasma parameters with different time scales.

Keywords: steady state, ECRH, ECCD, gas balance, impurity confinement, detachment

DOI: 10.1585/pfr.16.2402058

1. Introduction

Stellarators are ideally suited for stationary plasma operation because their magnetic confinement is mainly generated by external static magnetic fields and, in particular, they do not require any toroidal currents in the plasma to generate their rotational transformation and therefore the magnetic flux surfaces. The external magnetic fields also ensure the plasma stability and thus make an external permanent active position control of the plasma unnecessary.

The Wendelstein7-X (W7-X) stellarator has a superconducting coil system that generates a stationary magnetic field (shown in Fig. 1). It consists of 50 non-planar and 20 planar coils that allow a wide variety of magnetic configurations. In addition, it is equipped with further normal-conducting coils both inside and outside the plasma vessel, which are used for field error correction and fine adjustment. The inner plasma vessel is encased in a second vacuum vessel, the cryostat, which provides thermal insulation for the superconducting coils cooled with liquid helium. The plasma vessel is connected to the periphery by 256 ports. Through them the plasma heating, diagnostics and the cooling media are introduced into the plasma vessel [1].

The plasma forms a three-dimensional tube, which, depending on the magnetic configuration, is surrounded by 4 or 5 so-called magnetic islands with their own private flux surfaces as shown in Fig. 2. This structure enables the flow of energy and particles from the plasma to be directed to the so-called divertor, which are graphite tiles qualified for high heat load. The divertor surface cuts the islands

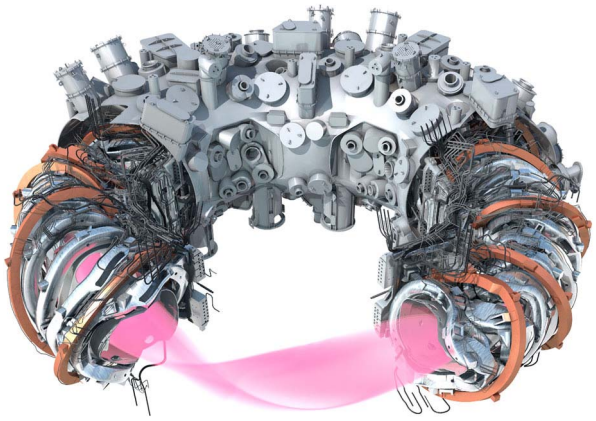

Fig. 1 W7-X plasma in the plasma vessel enclosed by the cryostat with the coils system. At outer surface of the cryostat there are the port feed troughs.

Fig. 2 Left: plasma shape with divertor structures. Right: poloidal cross section with edge island structure at different toroidal positions.

author's e-mail: laqua@ipp.mpg.de

*) This article is based on the presentation at the 29th International Toki Conference on Plasma and Fusion Research (ITC29).

so that strike lines arise on the plates that determine the position of the energy and particle flow.

The plasma vessel itself is equipped with additional graphite tiles. In areas with less power flow the plasma vessel surface is covered by panels made of stainless steel. In the experiments described here, the so-called test divertor unit (TDU) was used [2], It consisted of uncooled graphite tiles with a limited input energy.

W7-X also has the world's largest microwave heating system for plasma generation at the moment [3]. The electron cyclotron resonance heating (ECRH) works at a frequency of 140 GHz. That is twice the resonance frequency of the electrons with a magnetic field strength of 2.5 T, the nominal magnetic field of the superconducting coil system. The ECRH consists of 10 microwave sources, the so-called gyrotrons, with a unit power of up to 1 MW and an operating time of 30 minutes, which is also the targeted W7-X plasma duration of 30 minutes in the full completion phase.

The microwave beams are transmitted from the gyrotron to the W7-X machine in the atmosphere with the help of metallic mirrors as shown in Fig. 3. This so-called quasi-optical transmission enables a transmission efficiency of 93% with a transmission length of over 40 m and with 16 mirrors and 2 polarizers. The individual rays are initially bundled into up to 6 rays and transmitted together in an underground channel to the experimental hall using a large multi beam mirrors. Here the beams are separated again and radiated into the plasma vessel as individual rays. The atmospheric barrier is formed by vacuum windows made of polycrystalline diamond disks with a diameter of 106 mm. In the plasma vessel there are movable mirrors, so-called front steering launcher, which can launch the microwave beams in both a toroidal and a poloidal direction. A total of four front steering launcher are available for this purpose, each with up to 3 beams. Alternatively, two of the microwave beams can also be redirected to so-called remote steering launchers [4], components that are relevant for the fusion reactor. These are special microwave antennas which, based on the Talbot effect, can radiate the beams flexibly without moving elements in the plasma vessel.

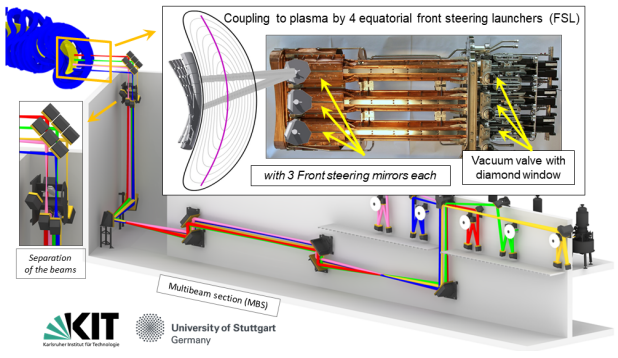

Fig. 3 ECRH-system with gyrotrons, individual beam, here colored for visibility, metallic mirrors and enlarged at the top the front steering launcher with movable mirrors at its front.

2. Steady State Operation

The term steady state must be considered in relation to the respective plasma physical quantities. Thus a plasma can be in equilibrium with regard to the energy confinement time, while its toroidal currents are far from being stationary. In this report, stationary plasmas are presented in relation to different plasma parameters.

The longest plasma discharge in the previous operation phase OP1.2 was 100 s long with an average density of $4{\cdot}10^{19}$ m^{-3}. It was sustained exclusively by 2 MW ECRH. As shown in Fig. 4, the discharge remained stationary for about 80 s.

The internal plasma parameters such as density and temperature did not change. However, the plasma facing components were far from equilibrium. The temperature at the uncooled divertor rose continuously to 900°C in the graphite and over 1200°C on the tile surface.

The increasing temperature led to outgassing of hydrogen bound in the graphite and, after 80 s, to a loss of density control. This also shows that the particle balance in this discharge does not reach equilibrium either. In Fig. 5 the different particle sources and sinks for this discharge are shown [5]. At the beginning, a lot of hydrogen gas has to be puffed in order to maintain the feed back controlled plasma density and to compensate for the particles absorbed at the walls or removed by the vacuum pumps.

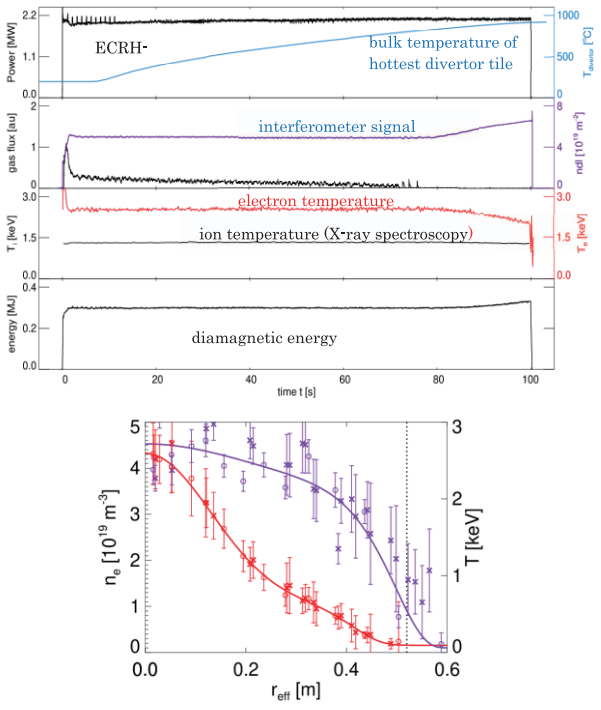

Fig. 4 Top: time traces of a 100 s plasma discharge. Bottom: the according electron density and temperature profile measured by Thomson scattering in the range of 20 - 40 s.

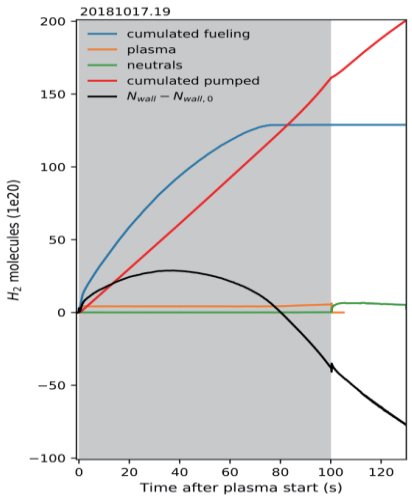

Fig. 5 Gas balance for the 100 s discharge.

With increasing time, the walls become saturated and the graphite tiles of the divertor, which are getting warmer and warmer, release more and more hydrogen. After around 80 s the pumping capacity of the walls and the vacuum pumps is no longer sufficient to absorb the amount of gas released from the divertor. Therefore, the plasma density increases, although no more gas is injected from the outside through the gas valves. It should be noted that previous long discharges reached this state after a shorter time and that there was a conditioning effect of the divertor tiles, so that less and less gas was released from discharge to discharge.

The next example of an equilibrium plasma is a high density discharge of $1.5{\cdot}10^{20}$ m^{-3}. This density could no longer be achieved with the well-absorbed ECRH with the X2 polarization. Rather, the less absorbed O2 polarization had to be used. Here the single pass absorption was only around 70 - 80%. It also depends on the square of the electron temperature. In order to improve the heating efficiency and to protect the machine from unabsorbed microwave power, special reflector tiles with holographic grids on their surface were installed opposite the ECRH launchers, which send the unabsorbed microwave rays through the plasma center [1]. There were further reflectors on the low field side in the plasma vessel, so that the rays propagated 3 times through the plasma and the cumulated absorption reached about 90% of the ECRH input power.

The high density discharge in Fig. 6 was sustained with only ECRH with O2 polarization and with a power of 6 MW. The plasma setup was carried out with 3 beams at X2 polarization. Their polarization was then turned to O2 during the discharge. The high density requirement made it difficult for the density control system to become stationary and the steady state was reached after 8 s first. The fluctuation of the density before steady state also led to a fluctuation in the electron temperature. This, in turn, had a strong influence on the microwave absorption, which can

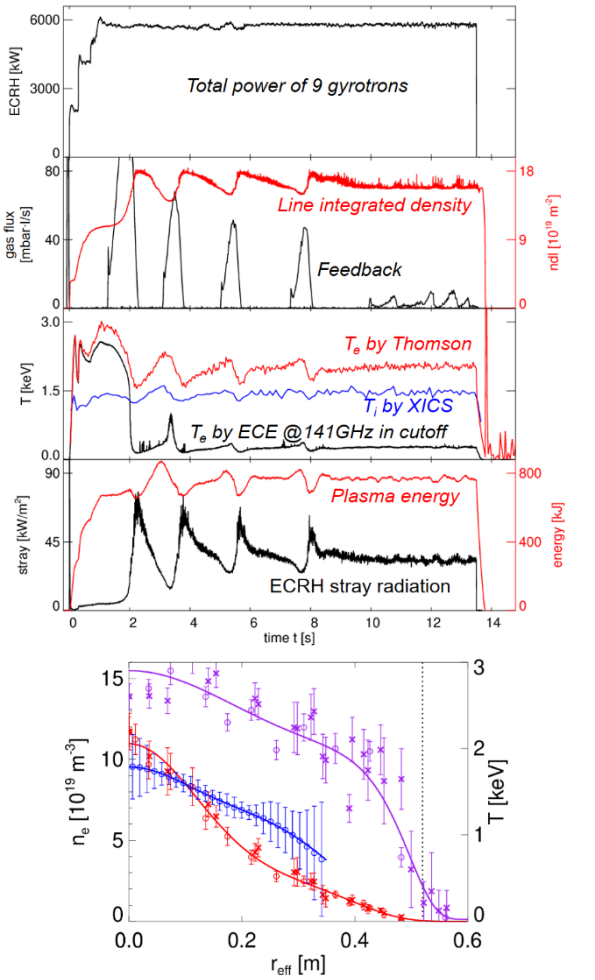

Fig. 6 Top: time traces of a high density discharge with pure O2 ECRH above the X2-cutoff density. Bottom: according electron density and electron and ion temperature profiles in the steady state phase.

be seen in the high fluctuation of the ECRH stray radiation, a measure of the non-absorbed microwave power.

Finally, the plasma remains in steady state for 5 s and the discharge had to be terminated regularly in order not to thermally overload the plasma-facing components.

Another characteristic parameter for reaching the steady state is the toroidal plasma current. As already mentioned, the W7-X stellarator does not require a toroidal plasma current for magnetic confinement. However, with certain magnetic configurations, a self-generated pressure-driven toroidal plasma current, the bootstrap current, can arise. Depending on the plasma pressure, this toroidal plasma current can reach values of up to about 80 kA and significantly change the rotational transform. Since the magnetic island structures are determined by the rotational transform, an uncontrolled plasma current can lead to a shift in the strike line on the divertor [6]. The intensive flow of power could then hit areas that are not adequately cooled and lead to damage.

The temporal development of the toroidal plasma cur-

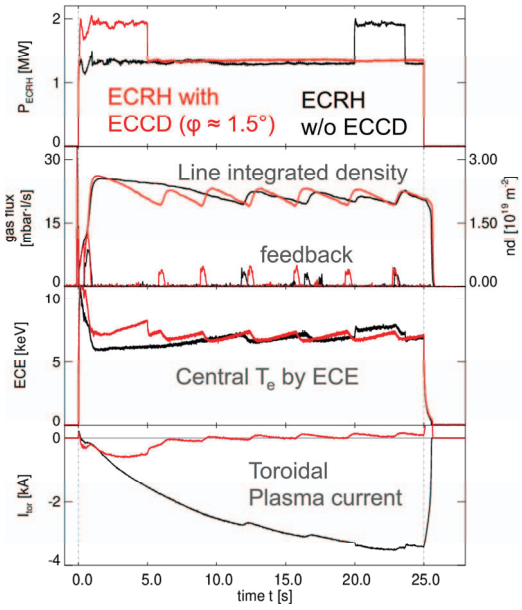

Fig. 7 Demonstration of Bootstrap current compensation by counter ECCD. In black: no ECCD and BS current only. In red: ECCD compensates BS current.

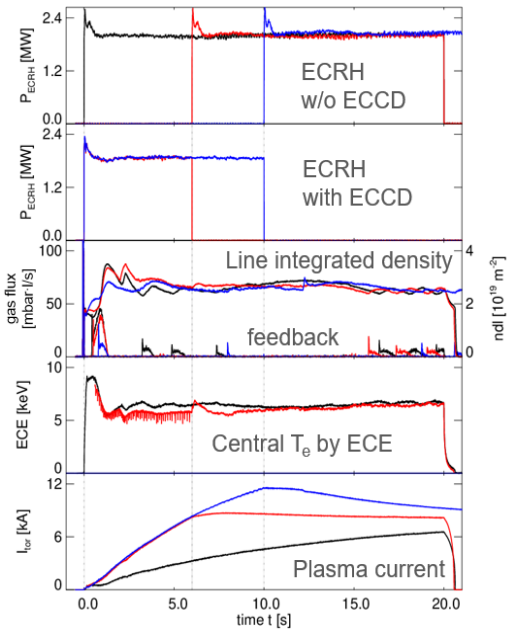

Fig. 8 Demonstration of a "boosted" transition to a stationary plasma current with co ECCD. In black: no ECCD and BS current only. In red and blue: with ECCD at the beginning.

rent is determined by the L/R time constant of the W7-X plasma, which is with 20 - 30 s two orders of magnitude larger than the energy confinement time.

There are two strategies for controlling the strike line position. In the first, the bootstrap current is permanently compensated by a counter-current generated by the electron cyclotron current drive (ECCD) with microwaves in the plasma. However, the ECCD current can only be generated with sufficiently high efficiency with the X2 polarization at densities below $1{\cdot}10^{19}\,\mathrm{m}^{-3}$. The second strategy aims to achieve the expected steady state current as quickly as possible with the help of ECCD. When the steady state current value is reached, the ECCD is replaced by pure ECRH, the plasma pressure is increased and the current is taken over by the bootstrap current.

In the Fig. 7 two experiments with red and black data tracks are shown. Initially, the plasma was operated without ECCD and the plasma current grew correspondingly slowly so that it did not reach its steady-state value even after 25 s. In the second discharge in red data tracks with the same ECRH power and density, a counter-directed toroidal plasma current was additionally driven with ECCD, which compensated for the bootstrap current.

Steady state conditions were achieved here immediately. It should be noted the in this experiment the magnetic field polarity was negative and therefore the Bootstrap current was also negative.

An experiment on the second strategy is shown in the Fig. 8. It was demonstrated here that the steady state for the plasma current can be reached much faster with an adapted ECCD. The data tracks for the case without ECCD are again in black, but this time in the positive polarity of the magnetic field the Bootstrap current developed in positive polarity with a long L/R time constant and the steady state was not reached even after 20 s. In a comparative discharge with red data traces, an additional current was driven with Co-ECCD in the direction of the bootstrap current in the first 6 s, so that the steady state value of the bootstrap current was reached within 6 s, after which the current drive was switched off and the bootstrap took over and remained in steady state. In a third discharge with blue data traces, the ECCD phase was extended to 10 s. Here the ECCD current exceeded the stationary bootstrap current and this then decayed with the corresponding time constant.

It should be noted, however, that high ECCD currents can lead to MHD instabilities that prevent a stady state. This is especially the case when the local ECCD changes the profile of the rotation transformation in such a way that it crosses a main rational number. This leads to repeated collapses of the central plasma temperature, especially with the rational number equal 1. The central temperature shown in Fig. 9. collapses within less than 10 µs [7].

Another characteristic time constant is the confinement time for plasma impurities with medium to high Z values. Here, the neoclassical calculations predict a confinement time of over 5 - 15 s, whereby it decreases with the atomic number Z. These long time constants would result in impurity accumulation if the sources were appropriately large. Experimentally, however, the values could not be confirmed [8]. Rather, that in the steady state ECRH plasmas the impurity confinement time was below 200 ms

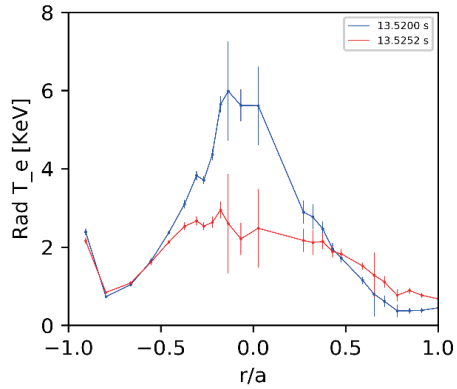

Fig. 9 Electron ECE radiation temperature profiles before (blue) and after (red) the MHD-driven central temperature collapse.

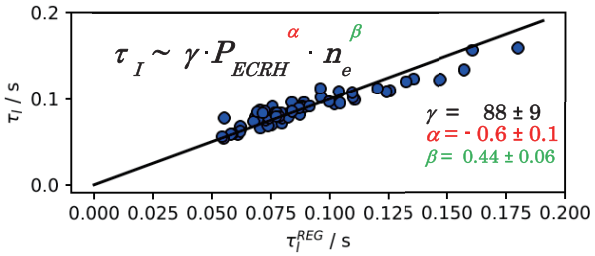

Fig. 10 Empirical scaling of the impurity confinement time for ECRH-plasma with gas fueling at W7-X.

and the expected Z-dependency could not be confirmed either. The experimental values were determined with the help of the so-called laser blow-off. Here the respective test material was shot into the plasma. The corresponding confinement time can then be determined from the decrease in time of the characteristic spectrum lines. The discrepancy between the measured values and those from neoclassical theory strongly suggests that the impurity transport was dominated by plasma turbulence. Initial turbulence calculations for the W7-X configurations confirm this assumption. Figure 10 shows the scaling for the impurity confinement for ECRH plasmas with gas flueling. It was determined from a large number of discharges with different density and heating power [9] and shows the expected negative power scaling ($\alpha = -0.6$) and positive density scaling ($\beta = 0.4$) of impurity confinement.

Finally, the energy and particle removal should also be considered. Charged particles that leave the last closed flow surface, follow the open field lines until they hit a divertor surface.

In the magnetic configurations of W7-X, the lengths of these field lines, the so-called connection lengths, can be very long with several 100 m. This is about an order of magnitude longer than in comparably large tokamaks. The diffusion perpendicular to the field lines leads to a broadening of the energy and particle flow and ultimately to a reduction in the power density on the divertor

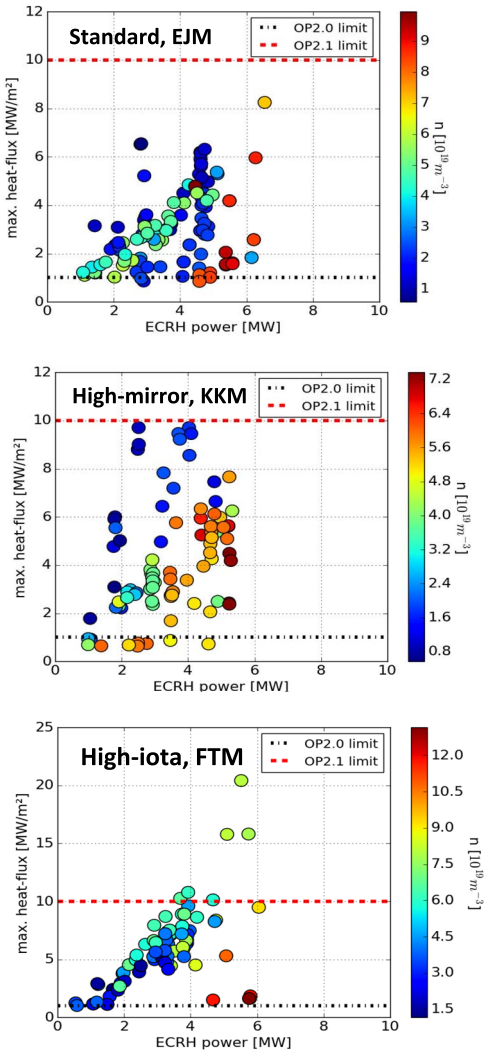

Fig. 11 Maximum heat load at the divertor surface as a function of ECRH power and electron density (color code) for the three most important magnetic configurations of W7-X.

plates. The intersection of the edge island with the divertor surface as shown in Fig. 2 and the connection length depends on the respective magnetic configuration. Therefore different power flux densities can occur. This is shown in Fig. 11. For the three most important W7-X configurations. The power flux density is shown as a function of the ECRH power and for different densities [10, 11]. In these experiments, the TDU divertor consisted of uncooled, thick graphite tiles that could absorb a high power density of up to 20 MW/m^2 for a short time, but were not suitable for steady state operation. For the cooled high heat load divertor in the next W7-X operation phase, it is necessary for steady state operation that the power density remains below its maximum steady state power density of 10 MW/m^2. While stead-state operation with up to 10 MW ECRH power appears to be possible for the EKM (standard) and also to a limited extent at higher densities for the KKM (high mirror) configuration, the load limit for the FTM (high iota) configuration is already reached at 5 MW

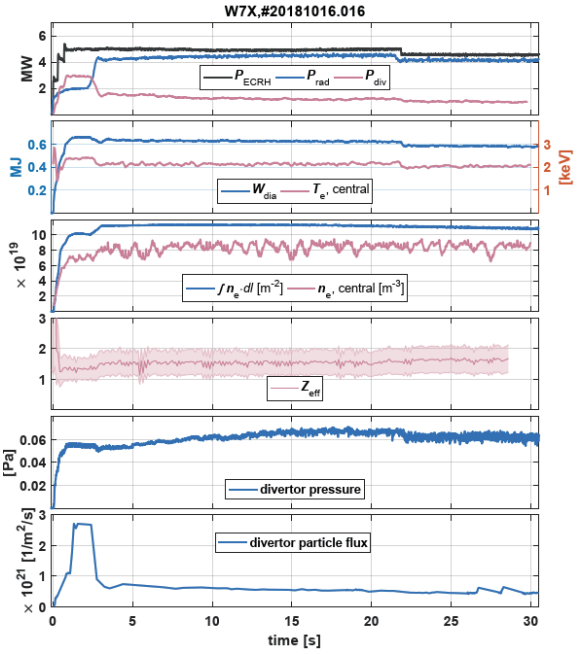

Fig. 12 Time traces of high ECRH power discharge with a steady state detachment phase of 26 s.

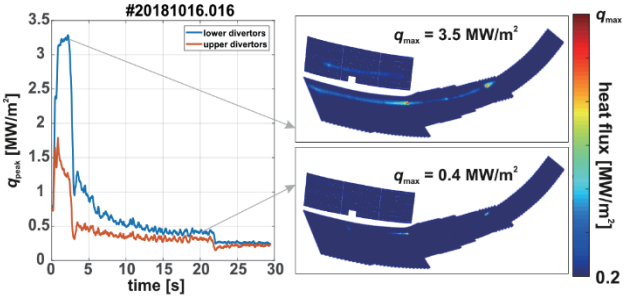

Fig. 13 Left: time traces of peak power density at the divertor. Right: Infrared pictures of the divertor for attached operation (top) and detachment (bottom).

heating power.

The power density on the divertor plates can, however, be strongly reduced by so-called detachment [11, 12]. A high density of neutral gas is built-up in front of the divertor plates, so that the flow of particles in the "gas cushion" in front of the divertor is completely stopped. The ions are decelerated and recombine at some distance from the divertor surface.

The recombination radiation is then radiated isotropically into the entire plasma vessel. At the same time, the constant flow of particles increases the neutral particle pressure in the divertor region and the particles can be pumped out more effectively. With the help of the detachment, steady state conditions could also be achieved for the TDU divertor. In the experiment shown in the Fig. 12 the transition to the detachment was reached at 3 s and the radiated power approached the heating power. The power flux on the divertor was reduced from 3.5 MW/m^2 to 0.4 MW/m^2 as shown in Fig. 13. This state could be kept stable for 26 s. The plasma was terminated regularly and no components had been at their power load limit.

3. Conclusion and Outlook

Various aspects of steady state operation were demonstrated on the W7-X stellarator. Due to the lack of complete cooling of the in-vessel components in the previous experimental phases, a completely steady state could not be achieved, but many of the plasma parameters were either in steady state or an extrapolation to steady state was possible.

In the next phase of the operation of W7-X, all in vessel components will be cooled sufficiently so that the goal of demonstrating stationary plasma operation with reactor relevant parameters should be achievable. Especially because the W7-X will be equipped with more powerful actors like the steady state pellet injector, the cryo-pump in the divertor region. Even though the cooled high heat load divertor is able to handle the expected power flux density up to 10 MW/m^2 at 10 MW heating power, the demonstrated stable steady state detachment operation opened a the operational window to more reactor relevant divertor scenarios. Therefore together with an expansion of the heating capacity by newly developed 1.5 MW gyrotrons a further improvement of its steady state performance is envisaged.

This work has been carried out within the framework of the EUROfusion Consortium and has received funding from the Euratom research and training program 2014-2018 and 2019-2020 under grant agreement No 633053. The views and opinions expressed herein do not necessarily reflect those of the European Commission

[1] T. Klinger *et al.*, Nucl. Fusion **59**, 112004 (2019).
[2] T.S. Pedersen *et al.*, Plasma Phys. Control. Fusion **61**, 014035 (2019).
[3] Erckmann *et al.*, Fusion Sci. Technol. **52**, 2, 291 (2007).
[4] W. Kasparek *et al.* EPJ Web of Conferences 87, 04004 (2015), DOI: 10.1051/epjconf/20158704005
[5] G. Schlisio *et al.*, Nucl. Futon 2020 (submitted)
[6] Y. Gao *et al.*, Nucl. Fusion **59**, 106015 (2019), doi: 10.1088/1741-4326/ab32c2
[7] M. Zanini *et al.*, Nucl. Fusion **60**, 106021 (2020).
[8] A. Langenberg *et al.*, Phys. Plasmas **27**, 052510 (2020).
[9] A. Langenberg *et al.*, Plasma Phys. Control. Fusion **61**, 014130 (2019).
[10] H. Niemann *et al.*, Nucl. Fusion **60**, 016014 (2020).
[11] T. S. Pedersen *et al.*, Nucl. Fusion **59**, 096014 (2019).
[12] M. Jakubowski *et al.*, submitted to Phys. Rev. Lett. (2020).